Isothermal Recrystallization Behavior of Cold-Deformed Martensite in an Ultra-Low-Carbon Microalloyed Steel

A. Sabet Ghorabaei [1], M. Nili-Ahmadabadi *[2]

Advanced Phase Transformations Laboratory (APTL), School of Metallurgy and Materials Engineering, University of Tehran, Tehran 14395-515, Iran

Abstract

One of the most promising ways to produce a grain-refined microstructure in some steel materials is the thermomechanical processing route of subcritical recrystallization annealing of a cold-deformed martensite structure. In the present study, the microstructural evolutions and the associated recrystallization kinetics under various subcritical annealing heat treatment conditions are explored in an API X120 grade, advanced, High-Strength, Low-Alloy (HSLA) steel with an initial cold-deformed martensite microstructure. The steel sheet was the subject of a conventional cold rolling process for moderate true strain of 60% followed by isothermal recrystallization for different temperature-time combinations. Optical microscopy and scanning electron microscopy were used to characterize the microstructural evolutions, and the recrystallization kinetics was evaluated by hardness measurements with the aid of the Johnson-Mehl-Avrami-Kolmogorov (JMAK) relationship. The experimental results indicated that annealing at 948 K (675 °C) for 18 h is the optimum condition to achieve a grain-refined ferrite microstructure with an averaged grain size of 5.2 μm. The slow kinetics of recrystallization was also revealed by JMAK model as the Avrami exponent was calculated around one for all of the experiments. These observations are rationalized in part by the possible formation of microalloying elements carbides during the annealing process in association with the existence of the inhomogeneously deformed initial microstructure. This results in the appearance of a continuous regime for the recrystallization nucleation along with the sluggish movement of recrystallization fronts.

Keywords: Advanced HSLA steels; Thermomechanical processing; Martensite recrystallization kinetics; Grain refinement.

1. Introduction

Improving the strength while preserving the ductility characteristics of metallic materials for applications in arctic environments has always been a concern for physical metallurgist, and this issue may be well responded by the formation of fine grains throughout the microstructure in a grain refining process [1]. The technique of cold rolling and subsequent annealing of martensite is a state-of-the-art procedure that has successfully been conducted on several steels to produce fine-grained microstructures with outstanding strength-ductility combinations [2-5].

The formation of fine ferrite grains from a cold-deformed martensite microstructure has been explained through a type of continuous recrystallization mechanism [5]. In this mechanism, the lamellar substructure of the martensite collapses by strain energy effects, and spheroidization of the collapsed regions occurs by boundary tension forces to

**Corresponding author*
Tel: +98 21 8208 4163
E-mail: nili@ut.ac.ir
Address: Advanced Phase Transformations Laboratory (APTL), School of Metallurgy and Materials Engineering, University of Tehran, Tehran 14395-515, Iran
1. M.Sc.
2. Professor

reduce the interfacial energies. Finally, by further growth of the spheroidized regions, fine ferrite grains evolve as recrystallized martensite areas.

Recrystallization is a thermally activated process wherein recrystallized nuclei grow by the interface-controlled mechanism [6,7]. Since the thermodynamic driving force for recrystallization is the excess energies stored in the material, the distribution quality of the energies in the microstructure directly influences the nucleation and growth behaviors of recrystallized grains [6]. Moreover, due to the controlling growth mechanism of the nuclei, any factor that affects the mobility of growing fronts would revolutionize the resultant growth kinetics of recrystallization [7]. Accordingly, process-dependent factors such as recrystallization temperature and deformation mode accompanied by its severity in relation to material-dependent factors such as plastic strain distribution and carbide formation are of particular factors with complex interactions that influence a recrystallization process. Therefore, it would be worthwhile to study the recrystallization behavior of advanced, High-Strength, Low-Alloy (HSLA) steels under certain process-material conditions to obtain a better insight about the nature of recrystallization in these metallic materials.

In the present paper, the microstructural evolutions along with the resultant recrystallization kinetics during subcritical isothermal annealing of the cold-deformed martensite microstructures are investigated and discussed in detail using an ultra-low-carbon, microalloyed API X120 steel.

2. Experimental Procedure

2. 1. Alloy preparation and the thermomechanical route

The implemented API X120 grade HSLA steel, compliant to the API 5L-PSL 2 standard [8], was cast into a 5-kg ingot by the use of the Vacuum Induction Melting (VIM) technique. The chemical composition of the alloy was measured based on the ASTM E415-14 standard [9] with an Oxford Instrument Model Foundry-Master Pro Spark Atomic Emission Spectrometer (AES), the results of which are shown in Table 1.

The ingot was initially hot forged at 1323 K (1050 °C) for total true strain of 0.85 and subsequently homogenized at 1423 K (1150 °C) for 50 h in a tube furnace under the vacuum of approximately 1 × 10^{-3} mbar. The homogenized ingot was hot rolled conventionally for total true strain of 1.23 at initial temperature of 1423 K (1150 °C) and then cooled in air from final rolling temperature at 1223 K (950 °C) to produce a 6-mm steel sheet.

Fig.1 shows a schematic representation of the applied thermomechanical route in three consecutive steps for exploring the recrystallization behavior. At step one, the sheet was re-austenitized at 1323 K (1050 °C) for 15 min and then quenched in a brine bath consisting of 10 wt% NaCl [10] to form a solution-annealed, fully martensitic microstructure. At step two, cold rolling was carried out for total true strain of 60% using a GL 200 two-high rolling machine with a capacity of 2 tonnes and the flat roller diameter of 110 mm under the conditions of a rolling speed of 16 rpm and a thickness reduction rate of approximately 0.1 mm per each rolling pass. Subsequently, at step three the cold-rolled sheet was isothermally recrystallized at three different temperatures of 923 K (650 °C), 948 K (675 °C), and 973 K (700 °C) for various holding times ranging from 10 s to 54 h followed by brine quenching.

It should be noted that the implementation of moderate plastic straining in this study was based on the reported results in literature [3] claiming that intermediately cold-rolled samples represent adequate recrystallization retardation in the presence of carbides and a proper tensile strength-ductility combination after the recrystallization process. However, the evaluation of tensile properties was not the major goal of the present study. Additionally, due to the relatively low initial thickness

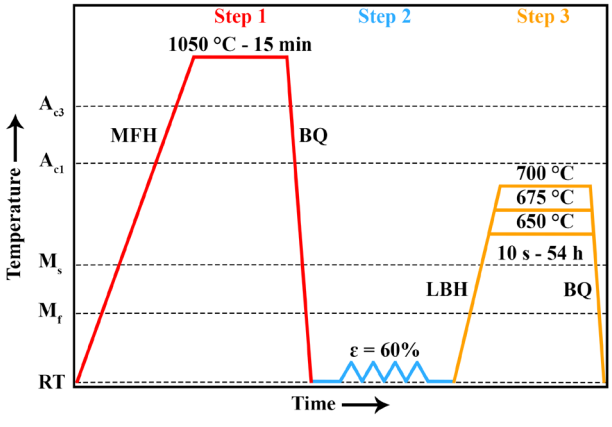

Fig. 1. A schematic illustration of the applied thermomechanical route in three consecutive steps for exploring the recrystallization behavior of cold-deformed martensite in the studied steel. MFH: Muffle Furnace Heating, LBH: Lead Bath Heating, BQ: Brine Quenching, A_{c1}: austenite-start temperature, A_{c3}: austenite-finish temperature, M_s: martensite-start temperature, M_f: martensite-finish temperature, RT: Room Temperature.

Table 1. The chemical composition of the studied steel (values are in wt.%).

C	Si	Mn	Cu	Ni	Cr	Mo	Ti	V	Nb	S	P	Fe
0.03	0.15	1.94	0.23	0.71	0.34	0.28	0.018	0.037	0.045	0.007	0.015	Balance

of the hot-rolled steel sheet, in order to prevent metallurgical difficulties during and after prolonged recrystallization annealing in a lead bath, the moderate plastic strain seemed to be more appropriate in this study.

2. 2. Microstructural characterization and kinetic evaluation

For general microstructural observations, several samples were machined from the sheet at each step of the thermomechanical process, and the metallography of the samples was carried out compliant to the ASTM E3-11 standard [11]. The polished surfaces of the samples were etched with a common Nital etchant solution of 2 vol.% HNO_3 and 98 vol.% C_2H_5OH [12], and a ZEISS Axioskop 2 MAT Optical Microscope (OM) along with an FEI Quanta 450 Scanning Electron Microscope (SEM) operating at an accelerating voltage of 20 kV was implemented to observe the microstructural characteristics of the samples.

To evaluate the kinetics of recrystallization, the volume fraction of recrystallized martensite was indirectly estimated by using a simple softening ratio as follows [13]:

$$S = (H_{CR} - H_{T,t})/(H_{CR} - H_{RX}) \quad \text{Eq. (1)}$$

, where S is the softening ratio that represents the volume fraction of recrystallized martensite (f_R), H_{CR} is the averaged hardness value of the cold-rolled samples, $H_{T,t}$ is the averaged hardness value of the cold-rolled samples after recrystallization annealing at a specific temperature (T) for a specific time (t), and H_{RX} is the averaged hardness value of the fully recrystallized samples. The Vickers macro-indentation measurement with a load of 30 kgf was conducted on the samples according to the ASTM E92-16 standard [14] by using an ESEWAY-DVRB.M hardness tester machine. The average of three measurements accompanied with the standard deviation was considered for the hardness result of each sample. Having the corresponding softening ratios, the isothermal recrystallization kinetics can be evaluated by using the Johnson-Mehl-Avrami-Kolmogorov (JMAK) equation as follows [6]:

$$f_R = 1 - \exp(-kt^n) \quad \text{Eq. (2)}$$

, where f_R is the recrystallized fraction, t is the annealing time in [s], k is a temperature-dependent coefficient, and n is the Avrami exponent, which depends on the mechanism of the nucleation event and the dimension and manner of the nuclei growth in the microstructures. It should be mentioned that the evaluation of recrystallized fraction by measuring the hardening variations has been confirmed to be a reliable approach with a good degree of accuracy (± 5%) in comparison to other microstructural characterization techniques such as Electron Back Scatter Diffraction (EBSD) analysis [15].

3. Results and Discussion

3. 1. Coarse-grained martensite and its response to cold deformation

Figs. 2(a) and (b) respectively illustrate typical OM and SEM micrographs from the microstructure of the studied ultra-low-carbon HSLA steel at the end of the first step of thermomechanical route (Fig. 1). A fully lath martensite microstructure is observed in the micrographs. Lath martensite is the prevalent martensite morphology in low-alloyed steels with carbon concentration of less than 0.6 wt. % [16]. According to the crystallographic features of lath martensite, the substructure of this microstructural constituent in a single prior austenite grain is hierarchically subdivided to characteristic parts, which are named as packets, blocks, and laths [17,18]. A typical martensite

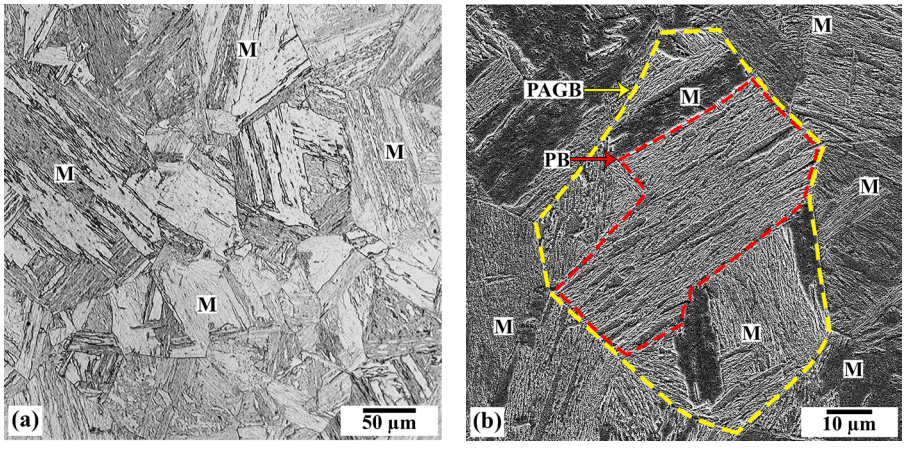

Fig. 2. Typical OM (a) and SEM (b) micrographs from the fully martensitic microstructure of the studied ultra-low-carbon HSLA steel resulting from the first step of the thermomechanical route. The micrographs illustrate coarse-grained lath martensite morphology with its characteristic, hierarchical substructure. M: Martensite, PAGB: Prior Austenite Grain Boundary, PB: Packet Boundary.

packet boundary is illustrated within a single, large prior austenite grain in the SEM micrograph (Fig. 2(b)), while the other hierarchical substructure features cannot be well discriminated in the micrograph due to low misorientation angles among the features.

The resulting micrographs from the cold-rolled martensitic samples are indicated in Figs. 3(a) and (b). After conducting 60% cold deformation on the martensite, an inhomogeneously deformed martensite structure is formed wherein some of the deformed regions are completely aligned with the rolling direction and some of them are relatively aligned by having a deviation angle with respect to the rolling direction. Conversely, there can be found some regions that represent the minimum response of the martensite constituent to the applied plastic strain. The aforementioned areas can be better distinguished in the SEM micrograph (Fig. 3(b)) where the three distinct regions of Fully Deformed Martensite (FDM), Semi-Deformed Martensite (SDM), and Partially Deformed Martensite (PDM) are typically shown in the microstructure. The PDM regions almost keep the initial morphology of lath martensite while the areas adjacent to the PDM regions are rigorously deformed, emphasizing that the PDM regions can act as strong deformation path deviators and barriers that may lead to the formation of SDM regions. These observations confirm the results of previous studies about the microstructural features of lath martensite after the cold deformation processing [2,3,5]. However, the observed inhomogeneous distribution of plastic strain in the microstructures can influence the recrystallization behavior of the deformed martensite and the associated distribution of recrystallized grains.

3. 2. Evolution of recrystallized martensite

Figs. 4(a), (b), and (c) show the microstructures of the cold-deformed martensite after isothermal recrystallization annealing at three temperatures of 923 K (650 °C), 948 K (675 °C), and 973 K (700 °C) for a selective set of annealing times of 54, 18, and 24 h, respectively. A combination of recrystallized martensite grains, i.e., ferrite, and large, non-recrystallized martensite regions can be identified in the microstructure of the samples after annealing at 923 K (650 °C) for a prolonged time of 54 h, indicating a low annealing temperature and, consequently, very slow recrystallization kinetics. By an increase in the annealing temperature to 948 K (675 °C), a recrystallized microstructure with an almost homogeneous distribution of fine ferrite grains is formed after 18 h of the isothermal heat treatment (Fig. 4(b)). However, by further increasing the annealing temperature to 973 K (700 °C), a relatively coarse-grained, recrystallized microstructure accompanied with an inhomogeneous distribution of ferrite grains is developed in comparison to the microstructures that evolve

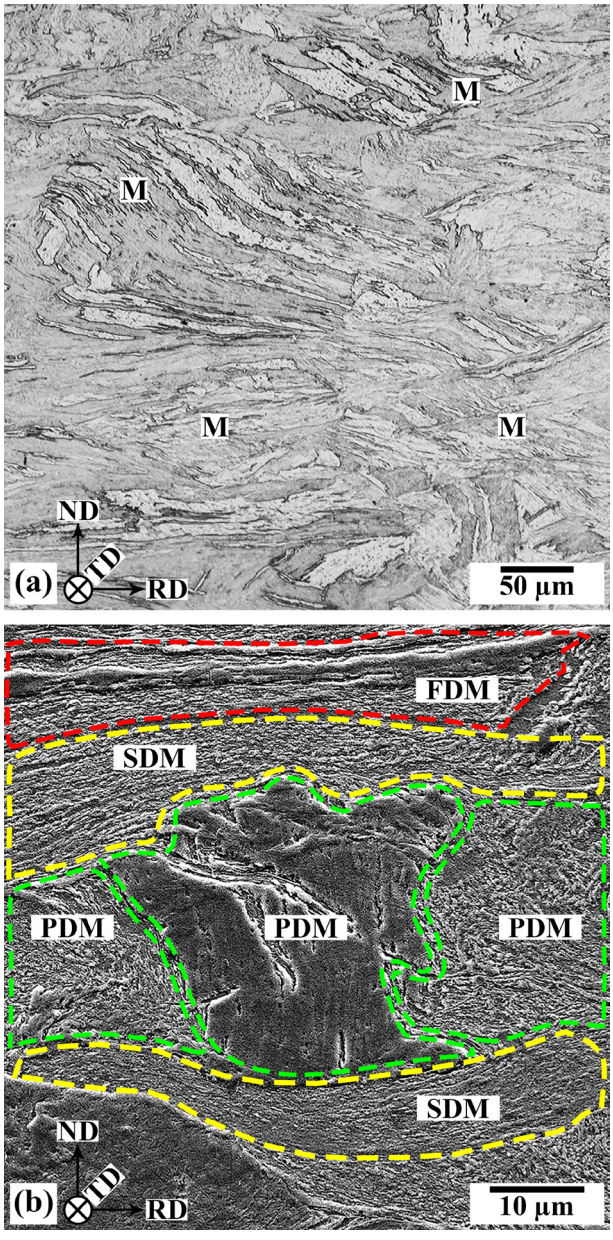

Fig. 3. Typical OM (a) and SEM (b) micrographs from the cold-deformed martensite microstructure resulting from the second step of the thermomechanical route. Three distinct regions in the microstructure can be identified after the deformation. M: Martensite, FDM: Fully Deformed Martensite, SDM: Semi-Deformed Martensite, PDM: Partially Deformed Martensite, ND: Normal Direction, RD: Rolling Direction, TD: Transverse Direction.

at 948 K (675 °C). As a result, the temperature-time combination of 948 K (675 °C)-18 h may be considered as suitable heat treatment conditions for recrystallization annealing in this study.

A typical microstructure of the partially recrystallized sample at 948 K (675 °C) for 6 h is illustrated in

Fig. 5(a). As indicated by arrows, very fine and relatively coarse growing ferrite grains can be characterized in the microstructure during the recrystallization process. Moreover, a large difference in the size of evolved ferrite grains can be also identified in the final size distribution of ferrite grains in the fully recrystallized samples at 948 K (675 °C) for 18 h (Fig. 5(b)), which may be related, in part, to variations in the velocity of recrystallization fronts. It should be stated that the distribution of ferrite grain size was evaluated by using the grain interception lengths method according to the ASTM E1181-02 standard [19], indicating a normal distribution of fine ferrite grains with an averaged grain size of 5.2 ± 0.3 µm accompanied with a relative accuracy of 6%.

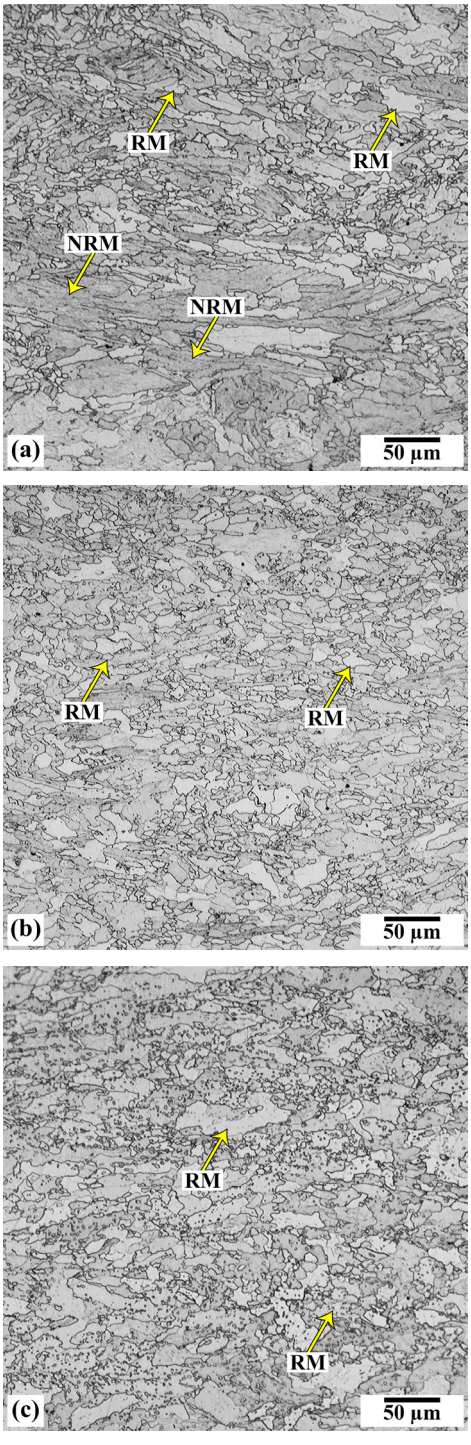

Fig. 4. Typical OM micrographs from the microstructural evolutions during isothermal recrystallization annealing of the cold-deformed martensitic samples for different temperature-time combinations of (a) 923 K (650 °C)-54 h, (b) 948 K (675 °C)-18 h, and (c) 973 K (700 °C)-24 h. The heat treatment conditions of (b) are considered as suitable annealing conditions in this study. RM: Recrystallized Martensite, NRM: Non-Recrystallized Martensite.

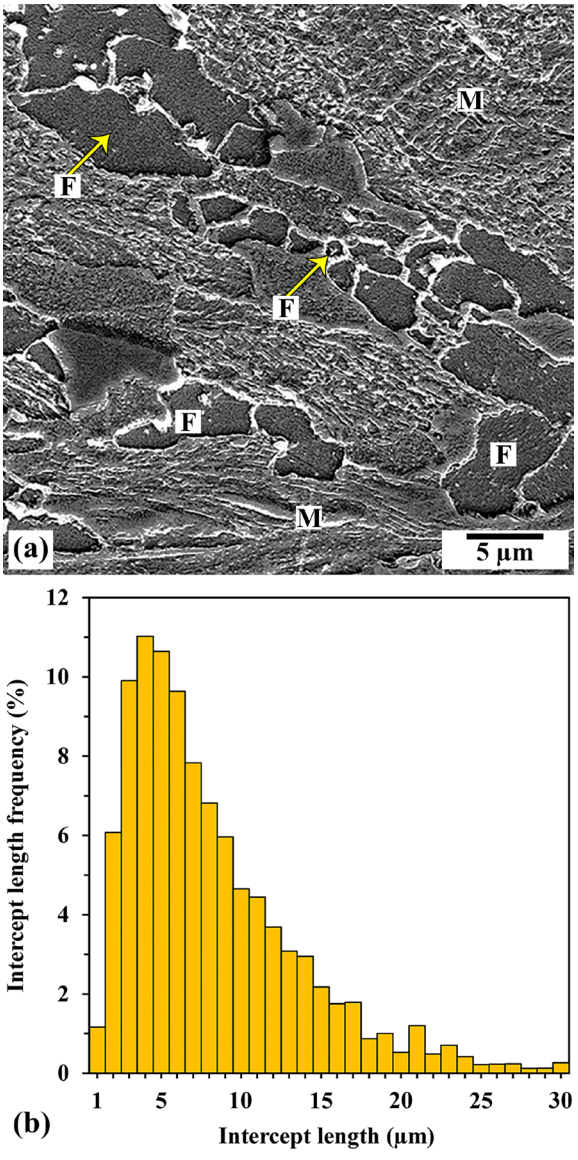

Fig. 5. (a) A typical micrograph from the microstructure of the samples partially recrystallized at 948 K (675 °C) for 6 h and (b) the distribution of ferrite grain size in the samples fully recrystallized at 948 K (675 °C) for 18 h. The observation of large differences in the size of evolved ferrite grains is noticeable from the beginning to the end of the recrystallization process. F: Ferrite, M: Martensite.

3. 3. On the slow kinetics of martensite recrystallization

According to Eq. (1), by having the values of H_{CR} and H_{RX} to be 307 and 175 HV_{30}, respectively, and by measuring the hardening variations and consequently softening ratios of the samples during the heat treatments, the kinetics of recrystallization can be evaluated by using Eq. (2), the results of which are shown in Figs. 6(a) and (b) and Table 2. For the three investigated temperatures, the Avrami exponent, n, is approximately equal to one and almost insensitive to the variation of annealing temperature. Conversely, by an increase of 50 K in the recrystallization temperature, the temperature-dependent coefficient, k, increases by more than 20 times in comparison to its low-temperature counterpart (Fig. 6(a) and Table 2). These results may indicate the slow growth kinetics of ferrite nuclei during the martensite recrystallization at annealing temperatures lower than 973 K (700 °C). As perceived from the JMAK model predictions in Fig. 6(b), the required times for having 95% of recrystallized martensite fraction at the annealing temperatures of 923 K (650 °C) and 948 K (675 °C) are approximately 76 and 12 h, respectively, while this time reduces to nearly 3 h at 973 K (700 °C). The process-dependent factors, i.e., the annealing temperature and the mode and severity of initial deformation, in relation to the material-dependent factors, i.e., the inhomogeneous distribution of plastic strain and the possible formation of microalloyed carbides in the microstructures, can significantly influence the nucleation behavior and resultant growth kinetics of ferrite grains during the cold-deformed martensite recrystallization.

Several studies have confirmed that the isothermal rate of martensite recrystallization increases by intensifying the severity of initial deformation due to an increment in the stored energy in the microstructures [3,20]. During cold rolling processing with its unique deformation mode, the distribution of plastic strain and resultant stored energy in the martensite microstructure would be locally different because of the existence of distinct crystallographic orientations in the martensite substructure and, consequently, distinct deformation paths [6,21]. The observation of three individual types of FDM, SDM,

Table 2. The values of fitting parameters in the JMAK model (Fig. 6(a)) for the martensite recrystallization indicating almost temperature-insensitive Avrami exponents and temperature-ultrasensitive coefficients.

Recrystallization temperature	Avrami exponent (n)	Temperature-dependent coefficient (k)
923 K (650 °C)	0.93	2.58×10^{-5}
948 K (675 °C)	1.08	3.03×10^{-5}
973 K (700 °C)	0.90	6.40×10^{-4}

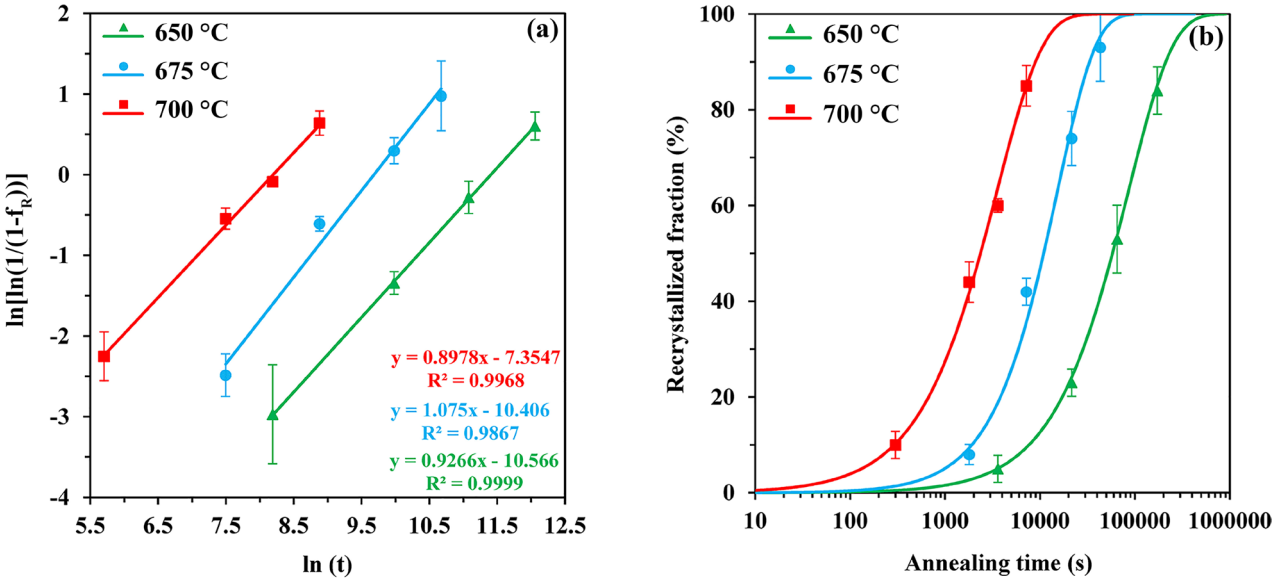

Fig. 6. The evaluating results of recrystallization kinetics for the annealed samples illustrating (a) the experimental data represented by the JMAK model in association with the fitted equation for each set of data and (b) the variation of ferrite volume fraction, resulting from the martensite recrystallization, with annealing time for the three investigated temperatures. The lines and curves represent the model results and the points indicate the experimental data along with corresponding standard deviations.

and PDM regions in the deformed martensite microstructure can be a direct consequence of the existence of specific deformation paths during cold rolling processing of the martensite constituent, the effects of which are expected to be more prominent in a coarse-grained initial microstructure (Figs. 2 and 3). Since the growth rate of recrystallized nuclei in high-energy regions would be much higher in comparison to low-energy counterparts, not only does the overall growth kinetics of the recrystallization process decrease by recrystallization of the high-energy regions but also the growth rate of newly recrystallized grains decreases through confinement and hard impingement with previously recrystallized grains. This situation is clearly observed from the beginning to the end of the recrystallization process, indicating large differences in the size of evolved ferrite grains (Fig. 5).

To further elucidate the material-dependent factors, thermodynamic predictions under ortho-equilibrium conditions for the alloy chemical composition (Table 1) were performed by using the console mode of Thermo-Calc 3.1 software with TCFE7 database. The calculations for a typical heat treatment temperature of 948 K (675 °C) indicated that complex microalloyed carbide precipitates, mainly consisting of (Nb,Ti)C and (Mo,V)C, can form with total volume fraction of 0.13% and equivalent chemical composition of Fe-14.46 C-0.05 Mn-1.75 Cr-11.73 Mo-16.23 Ti-14.93 V-40.53 Nb (all values in wt%) during the recrystallization annealing. These calculations are reasonably in accordance with the experimental studies published elsewhere [22].

In microalloyed steels with the capability of formation of precipitates, complex interactions between precipitation and recrystallization can occur that are generally as follows [23]: 1) decreasing a number of nucleation sites of precipitates and the rate of precipitation and postponing the process by annihilation of deformation dislocations during recrystallization; 2) sluggish movement or stagnation of recrystallization fronts through imposing Zener pinning forces on the interfaces by a fine and homogeneous distribution of precipitates; and 3) sluggish movement or stagnation of recrystallization fronts by the solute-drag effect of precipitating and non-precipitating components in solid solution. Among the alloying elements of the studied steel, Nb is known as a remarkable microalloying element both in the form of a precipitate and in the case of solid solution for decelerating and postponing the recrystallization kinetics. However, Mn and Mo are kinds of alloying elements that have much more stronger influence on decreasing the recrystallization kinetics in solid solution condition [23-25].

In the simple JMAK model, the temperature-dependent coefficient, k, represents the nucleation and growth rates of recrystallized grains [7]. Therefore, it is expected that under normal conditions by increasing the annealing temperature the value of increases, accordingly (Table 2). Conversely, the Avrami exponent, n, is reported to be a temperature-independent parameter that represents the governing nucleation mechanism and the dimension and manner of the nuclei growth, the value of which generally ranges from 0.5 to 4 [20]. In the present study, the Avrami exponent is approximately equal to one for the three investigated temperatures (Table 2). If the nuclei growth is hindered by different microstructural barriers such as Zener pinning forces and solute-drag effects, substantial changes occur in the manner of growth that result in a reduction in the growth dimension leading to a significant decrease in the Avrami exponent [6]. Furthermore, the inhomogeneously deformed initial microstructure having spatially and temporally different driving forces for recrystallization would represent a continuous nucleation mechanism at a constant temperature. This can also be expected to negatively affect the Avrami exponent, rationalizing in part the resultant slow kinetics of recrystallization (Figs. 3, 5, and 6).

From an industrial point of view, conducting the studied thermomechanical route on the API X120 steel may not be applicable due to the prolonged recrystallization annealing time and its related economic costs. Therefore, it might be necessary to further investigate the effects of material- and process-dependent factors on the recrystallization and precipitation kinetics to optimally design the thermomechanical process.

4. Conclusions

In this work, the recrystallization behavior of the cold-deformed martensite microstructure has been explored under various isothermal heat treatment conditions in an API X120 grade, ultra-low-carbon, microalloyed steel, and the associated conclusions are as follows:

- The fine-grained ferrite microstructure with an averaged grain size of 5.2 μm is produced by subcritical recrystallization annealing of the 60%-cold-deformed martensite microstructure at 948 K (675 °C) for 18 h.
- The evaluation of recrystallization kinetics by the JMAK model indicates that the Avrami exponent, n, is temperature-insensitive and approximately equal to one for the three investigated temperatures while the temperature-dependent coefficient, k, increases by more than 20 times when the annealing temperature increases just by 50 K. These results respectively emphasize the existence of a constant governing nucleation mechanism for all the experiments and the nucleation and growth rates of recrystallized grains that are enhanced by increasing the heat treatment temperature.
- The resultant slow kinetics of recrystallization accompanied with the observation of large differences in the size of evolved ferrite grains is partly rationalized by the possible formation of microalloyed carbide precipitates during the annealing process in association with the existence of the inhomogeneously

deformed initial microstructure. This results in the appearance of a continuous nucleation regime for the recrystallization process along with the sluggish movement of the growing fronts that is represented as a considerable reduction in the Avrami exponent in the JMAK model.

Data availability

The raw data required to reproduce the findings of this study are available from the corresponding author upon reasonable request.

Acknowledgements

Amir Sabet Ghorabaei would like to show his gratitude to Dr. Hassan Shirazi (University of Tehran, Iran) for assistance in casting the alloy and Dr. Hao Chen (Tsinghua University, China) for providing Thermo-Calc software.

References

[1] H. Halfa: J. Miner. Mater. Char. Eng., 2(2014), 428.
[2] R. Ueji, N. Tsuji, Y. Minamino, and Y. Koizumi: Acta Mater., 50(2002), 4177.
[3] R. Ueji, N. Tsuji, Y. Minamino, and Y. Koizumi: Sci. Tech. Adv. Mater., 5(2004), 153.
[4] H. F. Lan, W. J. Liu, and X. H. Liu: ISIJ Int., 47(2007), 1652.
[5] M. Najafi, H. Mirzadeh, and M. Alibeyki: Mater. Sci. Eng. A, 670(2016), 252.
[6] F. J. Humphreys and M. Hatherly: Recrystallization and Related Annealing Phenomena, Elsevier, UK, (2004).
[7] D. A. Porter, K. E. Easterling, and M.Y. Sherif: Phase Transformations in Metals and Alloys, CRC Press, USA, (2009).
[8] API Standard 5L-PSL 2: Specification for Line Pipe, American Petroleum Institute, USA, (2012).
[9] ASTM Standard E415-14: Standard Test Method for Analysis of Carbon and Low-Alloy Steel by Spark Atomic Emission Spectrometry, ASTM International, USA, (2014).
[10] ASM Handbook: Heat Treating, ASM International, USA, (1991).
[11] ASTM Standard E3-11: Standard Guide for Preparation of Metallographic Specimens, ASTM International, USA, (2011).
[12] ASM Handbook: Metallography and Microstructures, ASM International, USA, (2004).
[13] G. Liu, J. Li, S. Zhang, J. Wang, and Q. Meng: J. Alloy. Compd., 666(2016), 309.
[14] ASTM Standard E92-16: Standard Test Methods for Vickers Hardness and Knoop Hardness of Metallic Materials, ASTM International, USA, (2016).
[15] A. Karmakar, M. Ghosh, and D. Chakrabarti: Mater. Sci. Eng. A, 564(2013), 389.
[16] G. Krauss: Steels: Processing, Structure, and Performance, ASM International, USA, (2005).
[17] S. Morito, H. Tanaka, R. Konishi, T. Furuhara, and T. Maki: Acta Mater., 51(2003), 1789.
[18] H. Kitahara, R. Ueji, N. Tsuji, and Y. Minamino: Acta Mater., 54(2006), 1279.
[19] ASTM Standard E1181-02(2015): Standard Test Methods for Characterizing Duplex Grain Sizes, ASTM International, USA, (2015).
[20] Y. Mazaheri, A. Kermanpur, A. Najafizadeh, and A. Ghatei Kalashami: Metal. Mater. Trans. A, 47(2016), 1040.
[21] G.E. Dieter: Mechanical Metallurgy, McGraw-Hill, UK, (1988).
[22] J. Y. Koo, M. J. Luton, N.V. Bangaru, R.A. Petkovic, D.P. Fairchild, C.W. Petersen, H. Asahi, T. Hara, Y. Terada, M. Sugiyama, H. Tamehiro, Y. Komizo, S. Okaguchi, M. Hamada, A. Yamamoto, and I. Takeuchi: Int. J. Offshore Polar Eng., 14(2004), 10.
[23] S. Vervynckt, K. Verbeken, B. Lopez, and J.J. Jonas: Int. Mater. Rev., 57(2012), 187.
[24] N. Matsumura and M. Tokizane: Trans. Jpn. Inst. Met., 23(1982), 378.
[25] A. Ghatei Kalashami, A. Kermanpur, A. Najafizadeh, and Y. Mazaheri: Mater. Sci. Eng. A, 658(2016), 355.